

# Role of mixed-valence state in vanadium phosphates catalysts

V. Robert<sup>a,b</sup>, S.A. Borshch<sup>a,b,\*</sup>, B. Bigot<sup>a,b</sup>

<sup>a</sup> *Institut de Recherches sur la Catalyse, UPR 5401 CNRS, 2, avenue Albert Einstein, 69626 Villeurbanne Cédex, France*

<sup>b</sup> *Laboratoire de Chimie Théorique, Ecole normale supérieure de Lyon, 46, allée d'Italie, 69364 Lyon Cédex 07, France*

Received 4 June 1996; accepted 3 October 1996

## Abstract

An analysis of the electronic structure of the vanadyl pyrophosphate surface is given when vanadium atoms in different valence states are simultaneously present. A tetrameric vanadium-oxygen cluster is proposed to model the catalytic active site. Possible path for the interaction of 2,5-dihydrofuran with a lattice vanadyl oxygen leading to the formation of maleic anhydride is considered. It is shown that account of structural relaxation in mixed-valence state is needed to properly describe active site.

*Keywords:* Vanadyl pyrophosphate; Mixed-valence; Electronic structure

## 1. Introduction

The variety of stable oxidation states of transition metal ions is believed to be an important factor for catalytic activity of transition metal oxides [1]. If a solid or a cluster contain simultaneously metallic ions of a same element in different oxidation states, one deals with a mixed-valence system. The distribution of valences and accompanying structural relaxation may be of crucial importance for the reactivity at the different sites on the surface. The different valences can be attributed to particular metal sites (localized valence) or several ions can be considered as having an averaged (delocalized) valence [2,3].

We recently studied the role of mixed-valence

state in trimeric iron-oxygen clusters depicted in iron phosphates and acting as active sites in the catalysis of oxidative dehydrogenation of isobutyric acid [4]. Structure relaxation of this cluster favors the delocalization of excess electron between the central and one of the terminal octahedra of the cluster. Reduction of initially homovalent cluster occurs under adsorption of a molecule of isobutyric acid. The delocalization of excess electron allows intramolecular electron transfer to a ferric site of the same cluster where the OH group is coadsorbed. The mechanism of the intramolecular electron transfer singles out trimeric cluster from similar, yet more extended, systems also studied experimentally [5]. In the latter, the electron delocalization covers a higher number of sites and a smaller part of the excess electron density is accessible for interaction with an adsorbed

\* Corresponding author.

molecule. In contrast, the extra electron in dimeric cluster is almost strictly localized at one center.

Another example of mixed-valence systems appears in the heterogeneous catalysis of selective oxidation of *n*-butane. Vanadyl pyrophosphate  $(VO)_2P_2O_7$  is known to be the active and selective phase for the oxidation of *n*-butane into maleic anhydride [6–8]. It formally contains vanadium ions in the oxidation state +IV. However, experimental studies showed that partial oxidation of  $V^{IV}$  exposed to oxygen occurs in the initial step of active phase preparation [9]. Moreover, the formation of maleic anhydride requires the participation of  $V^{IV}$  and  $V^V$  sites in a sufficiently close vicinity [10]. The presence of  $V^{IV}-V^V$  mixed-valence pairs in the calcined catalysts was confirmed by XRD, FT-IR, EPR and EXAFS techniques [11].

Till now, the most complete study of maleic anhydride formation on a vanadyl pyrophosphate surface was done by Schiøtt et al. [12] (see also Ref. [13]). However, they only considered homovalent (tetra- or pentavalent) one-layer clusters and chains to model the surface.

In the present communication, we would like to study the role of mixed-valence state in the heterogeneous catalytic oxidation of butane. The trans-bipyramidal  $V_2O_8$  cluster unit (Fig. 1a) often completed by adjacent  $PO_4$  tetrahedra is usually chosen to represent the (010) surface of

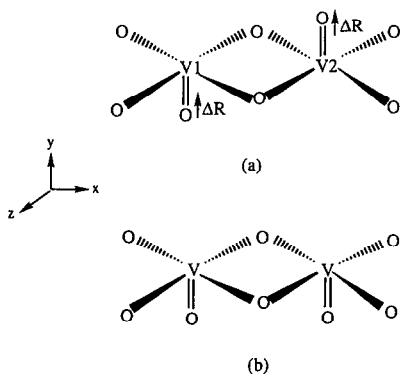


Fig. 1. Dimeric vanadium-oxygen clusters: (a) trans-bipyramidal unit.  $\Delta R$  characterizes the asymmetric distortion involving the two trans vanadyl groups; (b) cis-bipyramidal unit.

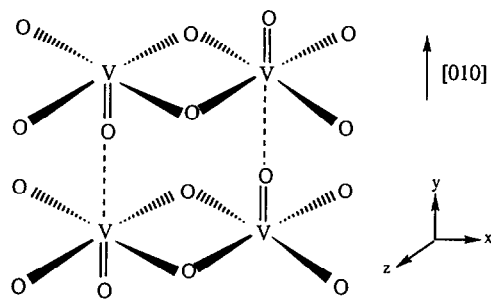


Fig. 2. Tetrameric vanadium-oxygen cluster.

vanadyl pyrophosphate. However, some recent data seem to indicate that presence of  $V^V$  is linked to the reorientation of vanadyl groups leading to cis- $V_2O_8$  cluster (Fig. 1b) [14]. Moreover, the participation of a few sublayers thanks to an oxygen atoms diffusion process has been supported by  $^{18}O$  labelling studies [15]. Besides, our preliminary ab initio calculations showed that excess electron in the trans- $V_2O_8^{-7}$  clusters is likely to occupy a  $d_{yz}$ -orbital, reflecting the vanadyl  $V=O$  group sensitivity to oxidation state changes [16]. The simplest model accounting for the coupling within  $V=O \cdots V$  stacks consists of a tetrameric vanadium-oxygen cluster (Fig. 2). Earlier we studied the charge distributions and structural relaxation in such mixed-valence clusters with different ratios  $V^{IV}:V^V$  [17]. We were here concerned with the catalytic properties of these clusters. However, the mechanism of the reaction considered below differs from that studied in Ref. [12]. The roles of lattice and chemisorbed oxygen in the selective oxidation of *n*-butane are still far from clear. Recent experimental results have shown that only lattice surface oxygen atoms were active in the formation of maleic anhydride [15]. So, we considered the adsorption of dihydrofuran on mixed-valence cluster (Fig. 2) and possible attack of lattice electrophilic oxygen on the basis of an extended Hückel (eH) approach.

## 2. Calculation method

We used the ASED (atomic superposition and electron delocalization) version of the eH-

Table 1  
Atomic parameters<sup>a</sup>

| Atom | Orbital | $\xi_\mu$     | $\xi_\nu$     | $H_{\mu\nu}$ (eV) |
|------|---------|---------------|---------------|-------------------|
| V    | 4s      | 1.30          |               | -8.81             |
|      | 4p      | 1.30          |               | -5.52             |
|      | 3d      | 4.75 (0.4755) | 1.70 (0.7052) | -11.00            |
| O    | 2s      | 2.28          |               | -32.20            |
|      | 2p      | 2.28          |               | -14.80            |
| C    | 2s      | 1.63          |               | -21.40            |
|      | 2p      | 1.64          |               | -11.40            |
| H    | 1s      | 1.30          |               | -13.60            |

<sup>a</sup> The d-orbitals are given as linear combination of two Slater type functions, and each coefficient is followed in parentheses by the weighting coefficient.

method [18] which does take into account electrostatic core repulsion and enables to estimate bond lengths. This correction technique (Anderson theory) based on a two-body repulsive energy was included into the original eH program [19]. It was noticed that, since the electron interactions in the overlap regions are omitted, the binding energy curves are usually too deep. Nevertheless, the method is likely to predict reasonable bond lengths [20]. The diagonal matrix elements and orbital exponents for atoms are summarized in Table 1, whereas a modified weighted Wolfsberg–Helmoltz formula with a distance dependent coefficient [20] was used to approximate off-diagonal matrix elements. It should be pointed out that other parametrization may be found in the literature [21] but qualitative description we worked on is certainly not significantly modified. The possible charge redistribution process was examined in terms of Mulliken definition of atomic charges.

For some model systems, *ab initio* Hartree–Fock and DFT (density functional theory) calculations were also performed (see below).

### 3. Vanadyl pyrophosphate model

Let us start with the analysis of a clean vanadyl pyrophosphate. As it was shown earlier [12], the extended models and discrete clusters

with and without attached phosphorous groups give similar results for electronic characteristics of vanadium and oxygen atoms. We ourselves focused on the vanadium-oxygen framework, since we noticed that the structure which attaches PO<sub>3</sub> units modelling the pyrophosphates did not lead to any significant changes in the calculated equilibrium geometries and related charge redistributions between different vanadium sites in mixed-valence clusters. Bond distances and angles were taken as average values of experimental data [22]. We first analyzed the charge distribution in V<sub>2</sub>O<sub>8</sub> dimer (Fig. 1a) in mixed-valence state with total charge -7. The localization of an 'excess' electron at one site is due to the desymmetrizing distortions [2,3]. We limited ourselves to a single distortion involving the shortening of one and the lengthening of the other V=O bond. We found that the symmetric geometry is stable against this distortion. Therefore, both vanadium sites are in the same average oxidation state +4.5.

We were then concerned with symmetric geometries of tetrameric mixed-valence vanadium-oxygen clusters. These structures result from the binding of two V<sub>2</sub>O<sub>8</sub> dimers. Nevertheless, two additional weakly bound O<sup>2-</sup> ions O5 and O6 were included in our model (Fig. 3) to depict infinite chains along the [010] direction and to stress the experimentally observed oxygen mobility in this direction [15]. O5 atom can also represent the oxygen atom of 2,5-dihydrofuran molecule when the latter is adsorbed on the surface. One should note that the environment of each vanadium atom is very close one to another but minor differences appear in the second coordination spheres. Consequently, such a structure is convenient to study charge reorganization accompanying desymmetrizing distortions. Again, we only considered the oxygen atoms displacements along the V=O ··· V bond. Fig. 3 shows the distortion associated with electron trapping characterized by  $\Delta R_1$ ,  $\Delta R_2$  and  $\Delta R_3$ , and gathers geometric parameters. Three different electronic mixed-valence configurations were examined, namely

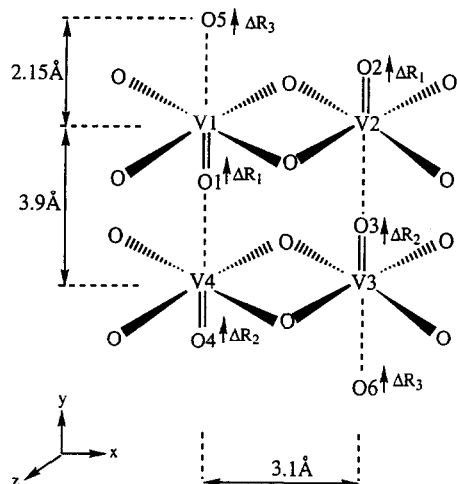


Fig. 3. Cluster structure used in molecular orbital calculations.  $\Delta R_1$ ,  $\Delta R_2$  and  $\Delta R_3$  are the three parameters defining the asymmetric distortion accompanying possible charge localization.

$d^0-d^0-d^0-d^1$ ,  $d^0-d^0-d^1-d^1$  and  $d^0-d^1-d^1-d^1$ , corresponding to different ratios  $V^{IV}:V^V$  and giving total charges  $-18$ ,  $-19$ ,  $-20$ , respectively. The system may be considered as a four  $d^0$ -center cluster belonging to symmetry group  $C_{2v}$ , with different numbers of 'excess' electrons. Reduction of the four- $V^V$  cluster is associated with filling of two quasi-degenerate orbitals (Fig. 4a) with one, two or three electrons. These non-bonding orbitals transform as  $A_1$  and  $B_2$  representations and they can mix with anti-

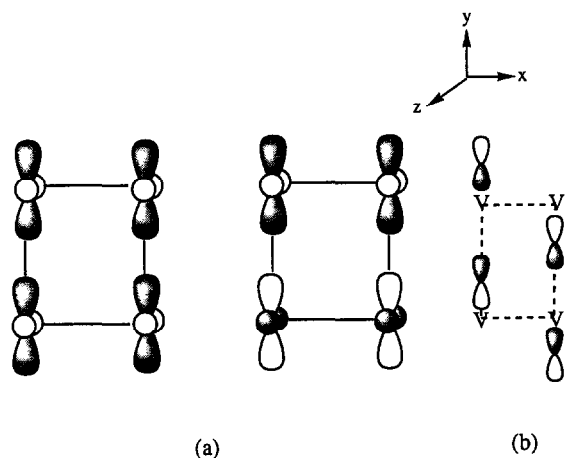


Fig. 4. (a) Non-bonding highest occupied molecular orbitals  $A_1$  and  $B_2$  in mixed-valent tetramer; (b) vacant  $B_1$  orbital of vanadyl oxygens.

Table 2

Vanadium charges at equilibrium geometry <sup>a</sup>

|    | $3V^V + 1V^{IV}$ | $2V^V + 2V^{IV}$ | $1V^V + 3V^{IV}$ | $4V^{IV}$   |
|----|------------------|------------------|------------------|-------------|
| V1 | 2.48 (2.43)      | 2.69 (2.66)      | 2.91 (2.88)      | 3.14 (3.10) |
| V2 | 2.36 (2.41)      | 2.59 (2.63)      | 2.81 (2.86)      | 3.04 (3.08) |
| V3 | 2.47 (2.43)      | 2.69 (2.66)      | 2.91 (2.88)      | 3.14 (3.10) |
| V4 | 2.36 (2.41)      | 2.59 (2.63)      | 2.81 (2.86)      | 3.04 (3.08) |

<sup>a</sup> In parentheses, the corresponding values for the symmetric geometry are given to stress the charge redistribution.

bonding orbitals of appropriate symmetry through distortions of vanadyl groups. As a general feature, all initial symmetric geometries were found unstable and equilibrium distances and vanadium charges are summed up in Tables 2 and 3. The  $V=O$  distances vary from 1.62 Å to 1.68 Å. Differences in  $V=O$  distances from 1.57 Å to 1.73 Å were also observed experimentally [22]. The calculated distortion transforms as  $A_2$  representation. Consequently, frontier orbitals  $A_1$  and  $B_2$  are likely to mix with mainly oxygen orbitals of  $A_2$  and  $B_1$  symmetries, respectively. The most suitable candidate for interaction is vacant  $B_1$  orbital (Fig. 4b) lying few electron-volts higher. This interaction is most efficient when HOMO is  $B_2$  orbital, i.e. electronic configuration  $d^0-d^1-d^1-d^1$  ( $3V^{IV} + 1V^V$ ).

Unlike in the dimer case, the electronic density varies from one vanadium atom to another. Charges analysis exhibits excess electron(s) localization on V1 and V3 atoms. Since  $|\Delta R_{1eq}| = |\Delta R_{2eq}|$ , 'cross-delocalization' (i.e. equal populations) between these two sites, as well as between sites V2 and V4, is observed. The

Table 3

Equilibrium parameters and distances (Å) <sup>a</sup>

| $(\Delta R_1, \Delta R_2)_{eq}$ <sup>b</sup> | V1-O1 | V2-O2 | V3-O3 | V4-O4 |
|--|-------|-------|-------|-------|
| $= (0.03, -0.03)$                            |       |       |       |       |
| Vanadyl group distances                      | 1.62  | 1.68  | 1.62  | 1.68  |

<sup>a</sup> The symmetric geometries ( $\Delta R_1 = \Delta R_2 = \Delta R_3 = 0$ ) correspond to a single value, 1.65 Å, for the vanadium-oxygen distances in the four vanadyl groups.

<sup>b</sup>  $(\Delta R_1, \Delta R_2)_{eq}$  stands for the equilibrium  $\Delta R_1$  and  $\Delta R_2$  parameters values and is found independent of the electronic configuration.  $\Delta R_3$  is found to be always equal to zero.

Table 4  
Overlap population and oxygen electronic charge <sup>a</sup>

| Geometry | Symmetric | Equilibrium |
|----------|-----------|-------------|
| V2–O2    | 0.787     | 0.752       |
| O2       | 7.24      | 7.31        |

<sup>a</sup> The variations of overlap population and oxygen electronic charge under geometry relaxation are similar for all electronic configurations.

shortening of V1–O1 and V3–O3 vanadyl group distances increases charge transfer displayed by the enhancement of charge density on V1 and V3 atoms. Therefore, interaction with adsorbed molecules is likely to occur on the Lewis acid site, namely V1, while O2 atom turns to be the most suitable for an electrophilic attack. As a matter of fact, a substantial decrease in the overlap population for the V2–O2 double bond is calculated while oxygen atom charge slightly increases (Table 4). Besides, one can assume that V4 bulk atom may also participate in the electrophilic attack since it can be easily oxidized as seen from ‘cross-delocalization’. Finally, the relative softness of the system displayed by  $(\Delta R_1, \Delta R_2)_{eq}$  may be a reflection of the lattice oxygen migration.

Our preliminary Hartree–Fock and DFT calculations led to very similar results for both binuclear and tetranuclear models [16]. We again observed delocalized electronic distribution for the former and localized one for the latter. Besides, equilibrium metal–oxygen distances are close to those found with the ASED method.

#### 4. 2,5-dihydrofuran oxidation

The detailed mechanism of maleic anhydride formation on a vanadyl pyrophosphate surfaces is still far from clear. It cannot be excluded that different structural units, including those containing phosphorous, may participate in different elementary acts of the reaction. We studied the role of mixed-valence state in the 2,5-dihydrofuran oxidative dehydrogenation which is proposed to be one of the possible steps of

catalytic reaction. Thus, we did not pay attention in our model to formation mechanism of this intermediate.

2,5-dihydrofuran molecule was built out of the MAD (molecular advanced design) code and geometrical parameters optimizations were then performed using ab initio SCF type calculations. It is observed that the four carbon and the oxygen atoms are almost coplanar. The adsorption was studied on vanadium–oxygen mixed-valence clusters with different electron countings and relaxed geometry described in the previous section.

We chose V1 atom as the adsorption site (Fig. 5). Therefore, the dihydrofuran oxygen substitutes for the weakly bonded oxygen O5. This adsorption site differs from that studied in Ref. [12] where adsorption occurred on V2 (Fig. 1a). In our geometry, the dihydrofuran molecule can interact with the vanadyl oxygen, thus allowing the participation of lattice oxygen as suggested in Ref. [15].

Additional optimizations of the dihydrofuran–V1 distance were performed leading to  $\Delta R_3$  equal to  $-0.03$  Å. Then, the question raised about the relative orientation of dihydrofuran ring relatively to the surface. The structure with the ring along the *y*-direction was found most stable as in Ref. [12]. However, the 90°-rotated ring conformation is less favorable by only  $\approx 0.5$  eV. From these calculations, no specific

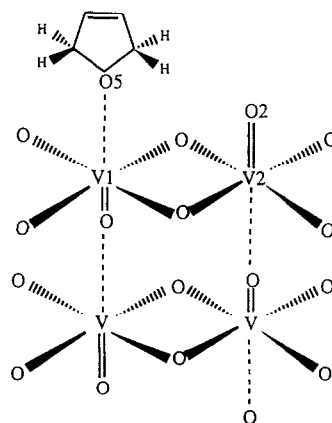


Fig. 5. Adsorption of 2,5-dihydrofuran on model catalyst.

conformation of 2,5-dihydrofuran ring could be chosen as the most favorable. Therefore, we concentrated on the conformation for which the O2-nearest neighbor hydrogen atom lies in *xy*-plan. The fragment molecular approach showed that 2,5-dihydrofuran fragment HOMO is likely to interact with low-lying antibonding d-orbitals of  $[V_4O_{19}]^{n-}$  ( $n = 18, 19, 20$ ) fragment (Fig. 6). By this interaction, the C–H bonding character of HOMO is reduced, leading to possible cleavage of this bond. Within the framework of our model, it can be then concluded that an O–H bond is expected to be made with participation of lattice oxygen. However, a rather large O–H distance (1.55 Å) was found and small O–H overlap population is observed ( $\approx 0.01$ ). More accurate calculations must be performed to get more realistic values.

We must mention one special feature directly linked to the mixed-valence state of our model tetramer. Up to now, the homovalent all  $V^{IV}$  electronic configuration has not been examined since  $V^V$  turned out to be required in the catalytic process. In terms of frontier orbitals interactions, we focused again on  $[V_4O_{19}]^{19-}$  fragment LUMO of  $d^0-d^0-d^1-d^1$  configuration ( $-10.6$  eV) and 2,5-dihydrofuran fragment HOMO ( $-12.5$  eV) (Fig. 7). Overlap between these two molecular orbitals is very small ( $\approx 0.001$ ). So, one can expect that the addition of an extra electron leading to a three-electron interaction and to  $d^0-d^1-d^1-d^1$  configuration is not destabilizing. However, any four-electron

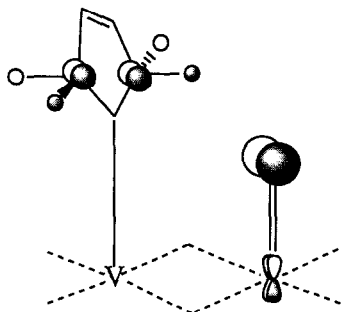


Fig. 6. 2,5-dihydrofuran HOMO ( $-10.5$  eV) interaction with low-lying antibonding d-orbitals of  $[V_4O_{19}]^{n-}$  cluster.

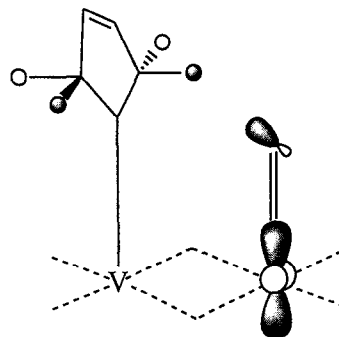


Fig. 7. 2,5-dihydrofuran HOMO interaction with  $[V_4O_{19}]^{19-}$  LUMO of  $d^0-d^0-d^1-d^1$  configuration ( $-10.6$  eV).

interaction is unfavored and this may be the reason why presence of about 25% of  $V^V$  appears to be optimal for stabilization of 2,5-dihydrofuran adsorbed on our model cluster.

## 5. Conclusions

This simplified quantum model enabled us to investigate the effects of simultaneous presence of  $V^{IV}$  and  $V^V$  ions in the vanadium pyrophosphate lattice. The account of several sublayers seems to be necessary to get an accurate description of the structural relaxation accompanying catalyst oxidation. On the basis of different considerations, a similar model was recently proposed [23]. Charge redistribution displayed 'cross-delocalization' between pairs of vanadium sites whereas bond lengths relaxation accounted for the observed softness of  $V=O \cdots V$  bond. For any electronic configuration, fragment molecular orbitals analysis showed that participation of lattice oxygen of vanadyl group has to be considered in the step of 2,5-dihydrofuran oxidation. Even if the reacting oxygen–hydrogen distance is large (1.55 Å) compared to usual O–H distances, this possible path for mechanism cannot be excluded.

Of course, the ASED method is too approximate to give reliable enough values of geometric parameters and charges. However, it is useful to depict the general trends in catalyst behavior. Besides, the whole space of possible

structural distortions should be studied. Full geometry relaxation would be the most appropriate way to precisely look into the role of lattice oxygen. But more sophisticated quantum-chemical calculations must be based on similar approaches in the description of mixed-valence state.

## Acknowledgements

We are grateful to M. Abon, J.-M. Millet and J.-C. Volta for helpful discussions.

## References

- [1] M. Witko, *J. Mol. Catal.* 70 (1991) 277.
- [2] D.B. Brown (ed.), *Mixed Valence Compounds* (Reidel, Boston, 1980).
- [3] K. Prassides (ed.), *Mixed valency systems: applications in chemistry, physics and biology* (Kluwer, Dordrecht, 1991).
- [4] V. Robert, S.A. Borshch and B. Bigot, *J. Phys. Chem.* 100 (1996) 580.
- [5] D. Rouzies, J.-M. Millet, D. Siew Hew Sam and J.-C. Vedrine, *Appl. Catal. A* 124 (1995) 189.
- [6] G. Centi, F. Trifirò, J.R. Ebner and V.M. Franchetti, *Chem. Rev.* 88 (1988) 55.
- [7] G. Centi, *Catal. Today* 16 (1993) 5.
- [8] H. Kung, *Adv. Catal.* 40 (1994) 1.
- [9] B.K. Hodnett, *Catal. Rev. Sci. Eng.* 27 (1985) 373.
- [10] Y. Zhang-Lin, M. Forissier, J.-C. Védrine and J.-C. Volta, *J. Catal.* 145 (1994) 267.
- [11] M. López Granados, J.C. Conesa and M. Fernández-García, *J. Catal.* 141 (1993) 671.
- [12] B. Schiøtt, K.A. Jorgensen and R. Hoffmann, *J. Phys. Chem.* 91 (1991) 2297.
- [13] J. Haber, R. Tokarz and M. Witko, *Proc. of the Symp. on Heterogeneous Hydrocarbon Oxidation, 211th ACS Meeting, New Orleans (1996)* p. 204.
- [14] P.T. Nguyen, N. Roberts, W.W. Warren and A.W. Sleight, *Abstr. of the 14th North American Meeting of the Catalysis Society, Snowbird (1995)*.
- [15] M. Abon, K.E. Béré and P. Delichère, *Catal. Today*, in press.
- [16] M. Bénard and V. Robert, unpublished.
- [17] V. Robert, S.A. Borshch and B. Bigot, *Chem. Phys.*, in press.
- [18] A.B. Anderson, *Int. J. Quant. Chem.* 49 (1994) 581.
- [19] P. Hermann, D. Simon and B. Bigot, *Surf Sci.* 350 (1996) 301.
- [20] A.B. Anderson, *J. Chem. Phys.* 62 (1975) 1187.
- [21] A.B. Anderson, S.Y. Hong and J.L. Smialek, *J. Phys. Chem.* 91 (1987) 4250; A.B. Anderson, *Chem. Phys. Lett.* 72 (1980) 514.
- [22] Y.E. Gorbunova and S.A. Linde, *Sov. Phys. Dokl.* 24 (1979) 138.
- [23] W.A. Goddard, III, F. Flaglioni, C. Brandow and C. Kankel, *Abstr. of the 6th Int. Conf. of Heterogeneous Catalysis, Tarragona (1996)* p. 13.